Analysis of Seismic Efficiency of the Electromagnetic Pulse Source "Yenisei"

Oxana V. Sadovskaya, Vladimir M. Sadovskii, Evgenii A. Efimov

EGU 2020-2754

Institute of Computational Modeling SB RAS
Department of Computational Mechanics of Deformable Media
Krasnoyarsk, Russian Federation

o_sadov@icm.krasn.ru, sadov@icm.krasn.ru, eugene6467@mail.ru

EGU General Assembly 2020

EGU 2020: Sharing Geoscience Online (#shareEGU20)

Online | 4 – 8 May 2020

Motivation

The northern territories of Eastern Siberia are characterized by a permafrost-taiga structure of the surface layer of soil, which reduces the efficiency of geological exploration using seismic sources of explosive and vibratory types.

Therefore, Geotech Holding Company developed a special eco-friendly electromagnetic pulse source "Yenisei", which seismic waves are the subject of analysis using high-performance computing in this presentation.

Seismic sources of the "Yenisei" series:
http://gseis.ru/en/our-business/field-seismic-works/impulse-technique/

Motivation

Electromagnetic source of seismic oscillations "Yenisei" is a non-explosive surface pulse seismic source with an electromagnetic actuator that contains one, two or four short-stroke electromagnets, working synchronously, with an autonomous power supply system from a capacitive storage of electric energy and a device for charging and discharging. The source exists in wheeled, sledge, mobile and water variants.

"Yenisei" is quite competitive in comparison with sources of explosive and vibrational types by efficiency and quality of exploration works, and it has undeniable advantages in the economical and environmental aspects.

The use of electromagnetic source "Yenisei" is incomparably cheaper, and it is almost the only possible means when working near buildings and constructions, in water protection zones and in areas where there are a lot of rivers and lakes. It is also applied on ice coverings of reservoirs, in shallow waters and on offshore.

The main goal of our research is to optimize the geometric and mechanical characteristics of the source based on mathematical modeling of the propagation of waves, generated by the source in layered soil massifs of complex rheology, with high resolution on supercomputers of cluster architecture.

Mathematical models and author's software codes

For this purpose, mathematical models, parallel computational algorithms and author's software codes were developed for analyzing wave processes in 2D and 3D formulations in geological media with various mechanical characteristics (viscoelastic soils, porous elastic-plastic rocks, granular materials with different resistance to tension and compression) of a layered-blocky structure [1, 2].

[1] *Sadovskaya O., Sadovskii V.* **Mathematical Modeling in Mechanics of Granular Materials.** Ser.: **Advanced Structured Materials**, Vol. **21**. Springer, Heidelberg – New York – Dordrecht – London, 2012. 390 p. `http://link.springer.com/book/10.1007/978-3-642-29053-4`

[2] *Sadovskii V.M., Sadovskaya O.V.* **Parallel Program Systems for the Solution of 2D and 3D Elastic-Plastic Problems of the Dynamics of Granular Media** (*2Dyn_Granular* and *3Dyn_Granular*). Certificates of state registration of the computer programs no. 2012613989 and 2012613990 from 28.04.2012 (Rospatent). **RU OBPBT 3**(80): 209. FIPS, Moscow, 2012. [in Russian]

Equations of the model in elastic blocks

It is assumed that the structure of a medium is known and represented by a set of heterogeneous blocks with curvilinear boundaries. Each block is characterized by its homogeneous material with corresponding governing equations.

In the simplest case of an elastic block, a system of equations of the linear dynamic elasticity, written in terms of velocities v and stresses σ, is fulfilled:

$$\rho\,\frac{\partial v}{\partial t} = \nabla \cdot \sigma, \quad \frac{\partial \sigma}{\partial t} = \rho\Big(c_1^2 - 2\,c_2^2\Big)(\nabla \cdot v)I + \rho\,c_2^2\big(\nabla v + \nabla v^*\big) \tag{1}$$

- ρ – density, c_1 and c_2 – velocities of longitudinal and transverse elastic waves
- ∇ – gradient over spatial coordinates, I – unit tensor
- asterisk denotes conjugate tensor, conventional notations of tensor analysis are used

The initial velocities and stresses are assumed to be zero. On a part of the boundary, external stresses caused by the action of concentrated load are preset. On the planes of symmetry, if any, the symmetry conditions are formulated. A part of the boundary can be a non-reflecting surface, on which the conditions for passage of waves without appreciable reflection are simulated. At the internal interfaces, the continuity conditions are set for vectors of velocities and stresses at the contact areas of the blocks.

Matrix form of systems for dynamic theory of elasticity and plasticity

The system of equations of dynamic elasticity is written in the following form:

$$A \frac{\partial U}{\partial t} = \sum_{i=1}^{n} B^i \frac{\partial U}{\partial x_i} + Q U + G \tag{2}$$

When taking into account the plastic deformation of a material,
the system (2) is replaced by the variational inequality

$$(\widetilde{U} - U)\left(A \frac{\partial U}{\partial t} - \sum_{i=1}^{n} B^i \frac{\partial U}{\partial x_i} - Q U - G \right) \geqslant 0, \qquad \widetilde{U}, \, U \in F \tag{3}$$

- F – convex and closed set, determined by the criterion of plasticity
- $U(t, x)$ – m-dimensional unknown vector–function, $\widetilde{U}$ – varied vector
- A – symmetric positive definite matrix of coefficients under time derivatives,
  B^i – symmetric matrices of coefficients under derivatives with respect to the spatial variables,
  Q – antisymmetric matrix, G is a given vector
- n – spatial dimension of a problem (1, 2 or 3)
- dimension m of the system (2) and concrete form of matrices–coefficients is determined
  by the used mathematical model

Matrix form of the systems for dynamic problems of granular and porous materials

In the problems of mechanics of granular media with plastic properties a more general variational inequality takes place

$$(\widetilde{V} - V)\left(A\,\frac{\partial U}{\partial t} - \sum_{i=1}^{n} B^i\,\frac{\partial V}{\partial x_i} - Q\,V - G \right) \geqslant 0, \qquad \widetilde{V},\ V \in F \qquad (4)$$

Vector–functions V and U are related by the equations

$$V = \varsigma\,U + (1 - \varsigma)\,U^{\pi}, \qquad U = \frac{1}{\varsigma}\,V - \frac{1 - \varsigma}{\varsigma}\,V^{\pi} \qquad (5)$$

Similar inequality describes dynamic behavior of porous materials taking into account the increase in stiffness after collapse of pores

- U^{π} is the projection of the vector of solution onto the given convex cone K, by means of which the different resistance of a material to tension and compression is described
- $\varsigma \in (0, 1]$ is the parameter of regularization of the model characterizing the ratio of elastic moduli in tension and compression

Structure of numerical algorithms

- The algorithm of numerical implementation of the variational inequality (4), having the most general form, is explicit in time and is constructed by means of the splitting method with respect to physical processes in the following way:

  - first, the elastic problem is solved at each time step
  - next, the obtained solution is corrected to take into account plastic, granular and porous properties of a material

- For the solution of elastic problem the two-cyclic splitting method with respect to the spatial variables is used

- One-dimensional hyperbolic systems of equations of the form

$$A \frac{\partial U^{(k)}}{\partial t} = B^i \frac{\partial U^{(k)}}{\partial x_i} + G^i \qquad (6)$$

$k = \overline{1, 2\,n}$ – number of the splitting stage, $i = \overline{1, n}$ – direction of splitting

in spatial directions are solved by means of the monotone finite-difference ENO–scheme of the "predictor–corrector" type; piecewise-linear splines, discontinuous at the boundaries of meshes, are constructed by a special procedure of limit reconstruction, which enables one to improve an accuracy of a numerical solution

- Plasticity, granularity and porosity of materials are taken into account by means of a special algorithms for the correction of stresses, used in computations

Two-cyclic splitting for the solution of elastic problem

The splitting method leads to a series of seven 1D problems, three of which are considered on the time interval $[t_n, t_n + \tau/2]$, and the last three on the interval $[t_n + \tau/2, t_n + \tau]$, where τ is the time step of grid:

$$A \frac{\partial U^{(1)}}{\partial t} = B^1 \frac{\partial U^{(1)}}{\partial x_1} + G^1, \quad U^{(1)}(t_n) = U(t_n)$$

$$A \frac{\partial U^{(2)}}{\partial t} = B^2 \frac{\partial U^{(2)}}{\partial x_2} + G^2, \quad U^{(2)}(t_n) = U^{(1)}(t_n + \tau/2)$$

$$A \frac{\partial U^{(3)}}{\partial t} = B^3 \frac{\partial U^{(3)}}{\partial x_3} + G^3, \quad U^{(3)}(t_n) = U^{(2)}(t_n + \tau/2)$$

$$A \frac{\partial U^{(4)}}{\partial t} = Q\, U^{(4)}, \qquad\qquad U^{(4)}(t_n) = U^{(3)}(t_n + \tau/2)$$

$$A \frac{\partial U^{(5)}}{\partial t} = B^3 \frac{\partial U^{(5)}}{\partial x_3} + G^3, \quad U^{(5)}(t_n + \tau/2) = U^{(4)}(t_n + \tau/2)$$

$$A \frac{\partial U^{(6)}}{\partial t} = B^2 \frac{\partial U^{(6)}}{\partial x_2} + G^2, \quad U^{(6)}(t_n + \tau/2) = U^{(5)}(t_n + \tau)$$

$$A \frac{\partial U^{(7)}}{\partial t} = B^1 \frac{\partial U^{(7)}}{\partial x_1} + G^1, \quad U^{(7)}(t_n + \tau/2) = U^{(6)}(t_n + \tau)$$

(7)

The vector–function $U^{(7)}(t_n + \tau)$ is a desired solution on the time layer $t_n + \tau$.

Structure of parallel program

Computational algorithms are implemented as parallel program systems for the solution of dynamic problems in structurally inhomogeneous deformable media (granular and porous materials, Cosserat continuum and multi-blocky medium) on multiprocessor computers by means of the SPMD technology in Fortran using the MPI library.

❶ Preprocessor program   Parallel program systems were registered in Rospatent.
- grid generation
- uniform distribution of initial data between parallel computational nodes
- packing of its part of data in binary files of direct access by each node of a cluster

❷ Main program
- step-by-step numerical computation of a problem on each node of a cluster
- data exchange between the processes
- special conservation of resulting data in the control points
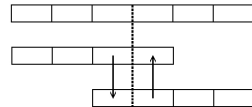
The scheme of exchange with contour meshes

❸ Postprocessor program
- compression of files, containing the results of computations in the control points
- graphical representation of results

Verification of the software was performed on exact solutions – formulas of geometric seismics for the hodographs of reflected and refracted waves.

# Examples of computations: Cover layers of clay, rock, water and ice

Let's consider 2-layered and 3-layered massifs of a medium of $60\,\mathrm{m} \times 40\,\mathrm{m} \times 40\,\mathrm{m}$. The upper 10-meter layer may be more compliant (clay) and, conversely, more rigid (rock) as compared with the lower 50-meter basic layer (ground). Besides, upper layer may be water. 3-layered medium consists of 3.5-meter layer from ice, 10-meter layer of water and thick layer of ground.
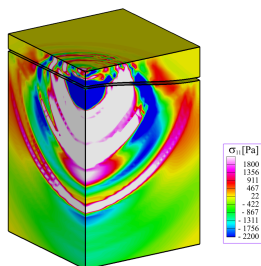
upper layer – **clay**,
lower layer – **ground**
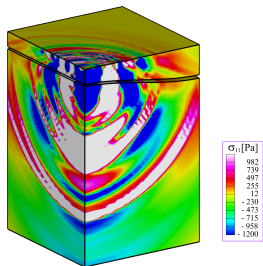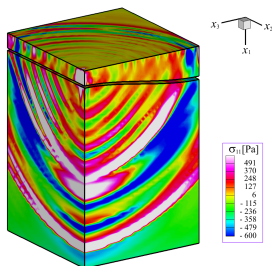
upper layer – **rigid ground**,
lower layer – **ground**

upper layer – **water**,
lower layer – **ground**

upper layer – **ice**,
middle layer – **water**,
lower layer – **ground**
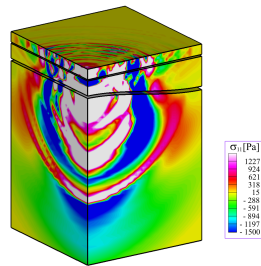
Level surfaces of normal stress σ_{11} in vertical direction ($t = 18\,ms$)

At the upper boundary of computational domain a localized action from the wheel source with 4 electromagnets is set. Taking into account the symmetry, computations are made for a quarter of the whole massif.

# Examples of computations: Cover layers of clay, rock, water and ice

On the left and right boundaries of computational domain the symmetry conditions are given.
Loading zone – a circle of area $1\,\mathrm{m}^2$ at the upper boundary, which is located near the boundaries of symmetry.

Computational domain is distributed uniformly between 96 computational nodes of a cluster: 16 nodes in the upper layer and 80 nodes in the lower one (2-layered case); 16 nodes in the upper layer, 16 nodes in the middle layer and 64 nodes in the lower layer (3-layered case). Each node of the cluster performs computations in parallel mode.
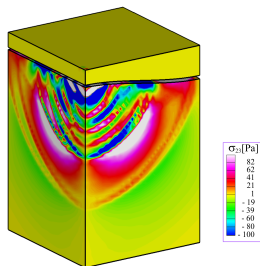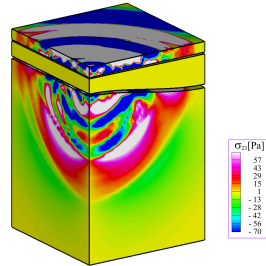
upper layer – **clay**,
lower layer – **ground**
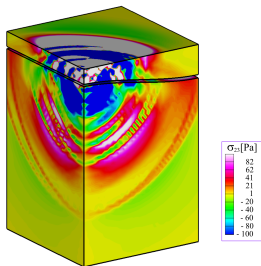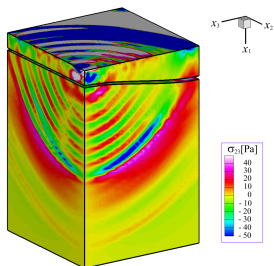
upper layer – **rigid ground**,
lower layer – **ground**

upper layer – **water**,
lower layer – **ground**

upper layer – **ice**,
middle layer – **water**,
lower layer – **ground**

Level surfaces of tangential stress σ_{23} in horizontal direction ($t = 18\,ms$)

Governing equations of the model for axisymmetric problem

If a seismic source is equipped with one electromagnet, and a geological medium is homogeneous and isotropic or has a plane-layered structure with homogeneous and isotropic layers of different density and rigidity, then a considered problem has axial symmetry. In this case, the equations become two-dimensional ones.

In the cylindrical coordinate system associated with the axis of symmetry x_1, passing deep into the massif through the center of the loading platform, and the radial axis x_2, directed along the daylight surface, they take the form:

$$\rho\, x_2\, v_{1,t} = (x_2\, \sigma_{11})_{,1} + (x_2\, \sigma_{12})_{,2}$$

$$\rho\, x_2\, v_{2,t} = (x_2\, \sigma_{12})_{,1} + (x_2\, \sigma_{22})_{,2} - \sigma_{33}$$

$$\rho\, x_2\, v_{3,t} = (x_2\, \sigma_{13})_{,1} + (x_2\, \sigma_{23})_{,2} + \sigma_{23}$$

$$\frac{1}{E}\,\sigma_{11,t} - \frac{\nu}{E}\,(\sigma_{22} + \sigma_{33})_{,t} = v_{1,1} - e_{11}^{vp}, \qquad \frac{1}{\mu}\,\sigma_{23,t} = v_{3,2} - \frac{v_3}{x_2} - e_{23}^{vp}$$

$$\frac{1}{E}\,\sigma_{22,t} - \frac{\nu}{E}\,(\sigma_{33} + \sigma_{11})_{,t} = v_{2,2} - e_{22}^{vp}, \qquad \frac{1}{\mu}\,\sigma_{13,t} = v_{3,1} - e_{13}^{vp}$$

$$\frac{1}{E}\,\sigma_{33,t} - \frac{\nu}{E}\,(\sigma_{11} + \sigma_{22})_{,t} = \frac{v_2}{x_2} - e_{33}^{vp}, \qquad \frac{1}{\mu}\,\sigma_{12,t} = v_{1,2} + v_{2,1} - e_{12}^{vp}$$

(8)

- e_{jk}^{vp} – components of a symmetric tensor of velocity of irreversible (viscous or plastic) deformation
- μ and ν – shear modulus and Poisson's ratio of a medium
- $E = 2\,\mu\,(1 + \nu)$ – Young's modulus

Energy balance equation

To obtain the energy balance equation, it is necessary to multiply each of three equations of motion on v_k $(k = 1, 2, 3)$, constitutive equations – on $x_2\,\sigma_{jk}$ with corresponding indices $j \leqslant k$, and after that the right and left sides should be summed up:

$$\left(\rho\,x_2\,\frac{v_1^2 + v_2^2 + v_3^2}{2} + W\right)_{,t} + D = (x_2\,v_j\,\sigma_{jk})_{,k} \tag{9}$$

- $D = x_2\,\sigma_{jk}\,e_{jk}^{vp}$ – dissipative power, non-negative at each point of a medium
- W – elastic potential

Elastic potential is a quadratic form relative to stresses:

$$2\,W = \frac{1+\nu}{E}\big(\sigma_{11}^2 + \sigma_{22}^2 + \sigma_{33}^2 + 2\,\sigma_{12}^2\big) - \frac{9\,\nu}{E}\,\sigma_0^2, \quad \sigma_0 = \frac{1}{3}\big(\sigma_{11} + \sigma_{22} + \sigma_{33}\big)$$

With a sufficiently wide choice of the equations of irreversible deformation for determining the values e_{jk}^{vp}, the system (8) refers to symmetric t-hyperbolic systems.

In the elasticity theory, when $e_{jk}^{vp} = 0$, the system splits into two independent subsystems.
First of them (equations with the numbers 1, 2, 4, 5, 6 and 9) describes motions in a plane passing through the axis of symmetry, and the second one (equations 3, 7 and 8) describes torsional motions.

Accounting for viscous properties

σ

E ν

λ_0 μ_0 η

σ
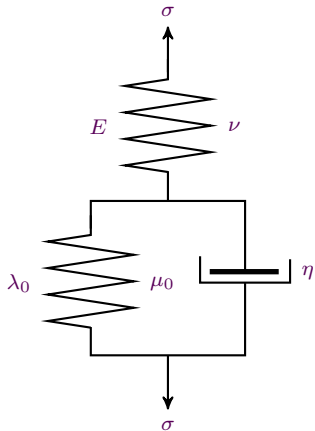
Rheological scheme
of a viscoelastic material

Viscous properties of a soil are taken into account
within the framework of the Poynting–Thomson model
of a viscoelastic medium, which in mathematical geophysics
is commonly called the standard geomaterial model.

Governing equations of irreversible deformation have the form:

$$e_{jk}^v = \frac{\sigma_{jk}' - s_{jk}'}{\eta}$$

$$\frac{\partial s_{jk}}{\partial t} = \lambda_0 \big(e_{11}^v + e_{22}^v + e_{33}^v\big)\delta_{jk} + 2\,\mu_0\,e_{jk}^v$$

- λ_0 and μ_0 – the relaxation Lame parameters
- η – viscosity coefficient
- s_{jk} – conditional stress tensor
- δ_{jk} – the Kronecker delta
- prime is used to denote the deviator components of tensors
  (in particular, $\sigma_{jk}' = \sigma_{jk} - \sigma_0\,\delta_{jk}$)

Accounting for plastic properties

To account for plasticity, the formulation of governing relationships of the flow theory is used in the form of variational inequality:

$$(\tilde{\sigma}_{jk} - \sigma_{jk})\, e^p_{jk} \leqslant 0, \qquad \tilde{\sigma},\ \sigma \in F \tag{10}$$

- F – set of admissible variations of the stress tensor
- $\tilde{\sigma}$ – an arbitrary element of F
- Einstein's rule of summation over repeated indices is applied

This variational inequality is a formulation of the von Mises principle of the maximum power of plastic dissipation.

If the point σ lies inside the set F, then, due to the arbitrariness of variation, from (10) follows a system of equations (8) describing the elastic process. If σ is a boundary point, then the associated law of flow is satisfied, according to which the plastic strain rate vector in the space of tensors is directed along the external normal to the boundary of F.

Boundary of the set F in the stress space – the yield surface of a material – is determined by the condition of plasticity. When modeling the irreversible shear strain, the von Mises–Schleicher plasticity condition is applied, taking into account the influence of hydrostatic stress σ_0 on the yield point of a soil: $\sigma'_{jk}\, \sigma'_{jk} = 2\,\tau_s - f_s(\sigma_0)$. To account for irreversible volumetric strain, an additional plasticity condition is used: $\sigma_0 = \sigma_s$ (σ_s – ultimate hydrostatic stress).

Under simultaneous consideration of viscous and plastic properties of a soil, the irreversible strain rates are equal to the sum of viscous and plastic components: $e^{vp}_{jk} = e^v_{jk} + e^p_{jk}$.

Seismic source efficiency

By integrating (9) over the spatial axisymmetric domain Ω, one can write the energy balance equation in integral form:

$$\frac{\partial}{\partial t} \int_{\Omega} \left(\rho \, \frac{v_1^2 + v_2^2 + v_3^2}{2} + W \right) d\Omega + \int_{\Omega} D \, d\Omega = \int_{\Gamma} v_j \, \sigma_{jk} \, n_k \, d\Gamma \tag{11}$$

- $d\Omega = x_2 \, dx_1 \, dx_2$ and $d\Gamma = x_2 \, d\gamma$ – spatial elements of the volume and the boundary of Ω
- $d\gamma$ – corresponding arc element
- n_k – projections of the external normal vector onto the coordinate axes ($n_3 = 0$)

The right-hand side of the equation (11) is the power flow through the boundary, which leads to a change in kinetic, potential and dissipative energy in this domain.

The seismic source efficiency is described as the ratio $\mathfrak{x}_i = E_i / E_0$ of the energy flux E_i through a circle of radius r_i at the depth h_i over time t_* (this energy can turn into the energy of waves reflected from the surface of a circle) to the energy E_0 of action of electromagnet on a soil mass through the platform of radius r_0:

$$E_0 = \pi \int_0^{t_*} p(t) \left(\int_0^{r_0} v_1(0, x_2, t) \, dx_2^2 \right) dt, \quad E_i = \pi \int_0^{t_*} \left(\int_0^{r_i} v_j(h_i, x_2, t) \, \sigma_{j1}(h_i, x_2, t) \, dx_2^2 \right) dt$$

The time t_* is chosen to be rather large compared with the time of action of the load from the pulse seismic source.

If the interfaces between layers are not plane ones or if nonlinear effects of plasticity are taking into account, then this approach is not applicable. In this case, it is necessary to carry out computations using 3D models.

Parameters of loading
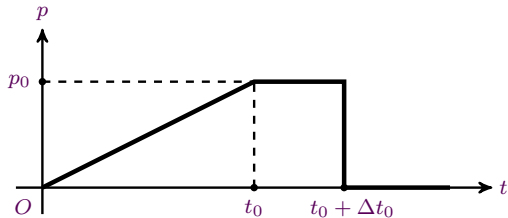
Graph of pressure from the source

The graph of pressure change, generated by a pulse seismic source "Yenisei", contains a region of monotone, close to linear, increase of pressure in the time interval t_0 from 5 to 10 ms, and a "tail" of constant pressure in the interval $\Delta t_0 \approx 2.5$ ms due to the constructional features of a seismic source. Then a sharp, almost instantaneous unloading takes place. The maximum pressure p_0 is determined by the energy of a pulse action.

The radius of a loading platform varies from $r_0 = 0.57$ to 0.8 m with a variation of the platform area from 1 to 2 m^2. At the stage of monotone loading, the soil part immediately adjacent to the platform, the so-called "added mass", accumulates elastic energy, which, when the pressure is released, generates a shock wave of unloading, propagating into the interior of a rock massif.

The hypothesis is that by the moment of unloading the seismic wave field in the considered range of times of active loading depends weakly on the value of t_0. Therefore, it is possible to consider t_0 as infinitely large value, and calculate the amplitudes and frequencies of excited waves based on the model of a static loading with instantaneous release of pressure.

Method of superposition (static problem)

Solution of a static problem is built according to the method of superposition by solving the Boussinesq problem on the action of a concentrated normal force on the boundary of an elastic half-space. The Boussinesq solution plays the role of the Green function in determining static stresses – initial conditions for solving the problem on instantaneous unloading based on the equations of dynamics of a geomedium. In the Boussinesq problem:

$$u_1^0 = \frac{1}{4\,\pi\,\mu}\left[2\,(1-\nu)\,\frac{1}{r} + \frac{x_1^2}{r^3}\right], \qquad u_2^0 = -\frac{1}{4\,\pi\,\mu}\left[(1-2\,\nu)\,\frac{x_2}{r\,(r+x_1)} - \frac{x_1\,x_2}{r^3}\right]$$

$$u_3^0 = -\frac{1}{4\,\pi\,\mu}\left[(1-2\,\nu)\,\frac{x_3}{r\,(r+x_1)} - \frac{x_1\,x_3}{r^3}\right], \qquad \sigma_{11}^0 = -\frac{3\,x_1^3}{2\,\pi\,r^5}, \qquad \sigma_{12}^0 = -\frac{3\,x_1^2\,x_2}{2\,\pi\,r^5}$$

$$\sigma_{22}^0 = -\frac{3\,x_1\,x_2^2}{2\,\pi\,r^5} - \frac{1-2\,\nu}{2\,\pi\,r^3}\left[\frac{r^2 - r\,x_1 - x_1^2}{r+x_1} - \frac{x_2^2\,(2\,r+x_1)}{(r+x_1)^2}\right]$$

$$\sigma_{33}^0 = -\frac{3\,x_1\,x_3^2}{2\,\pi\,r^5} - \frac{1-2\,\nu}{2\,\pi\,r^3}\left[\frac{r^2 - r\,x_1 - x_1^2}{r+x_1} - \frac{x_3^2\,(2\,r+x_1)}{(r+x_1)^2}\right]$$

- $r = \sqrt{x_1^2 + x_2^2 + x_3^2}$ – distance from the point of a medium to the origin of coordinates, in which a single concentrated force is applied

Displacements and stresses for an axisymmetric static state with distributed pressure are calculated by means of this solution using the convolution formula:

$$w(x_1, x_3) = p_0 \int_{-r_0}^{r_0} \int_{-r_0}^{r_0} H(\xi_2, \xi_3)\,w^0(x_1, x_2 - \xi_2, -\xi_3)\,d\xi_2\,d\xi_3$$

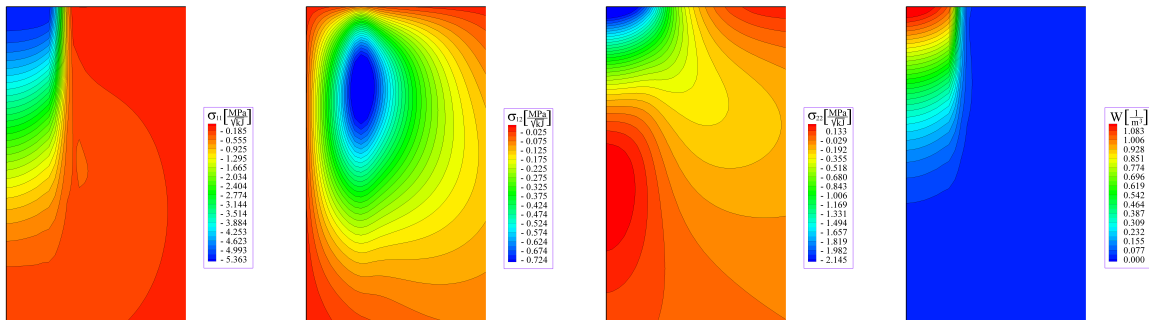- H – an indicator function ($H = 1$ inside the circle $\xi_2^2 + \xi_3^2 \leqslant r_0^2$, $H = 0$ – outside)

Computational results: Static problem
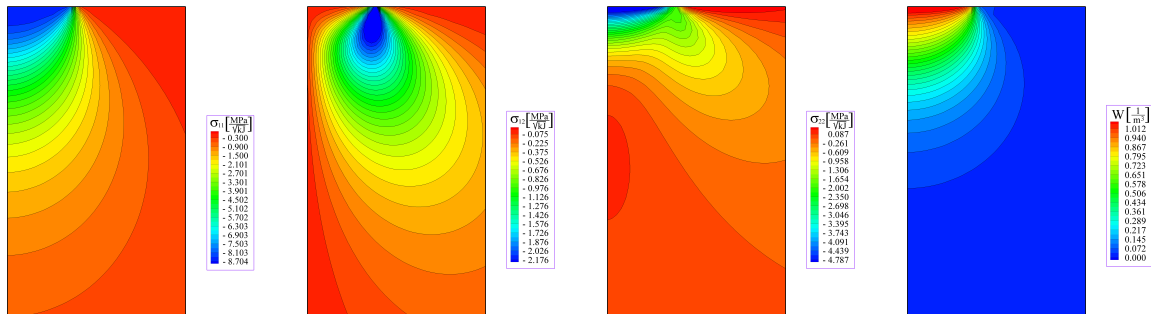
Level curves of static stresses σ_{11}, σ_{12}, σ_{22} and elastic energy W in the ground under loading platform
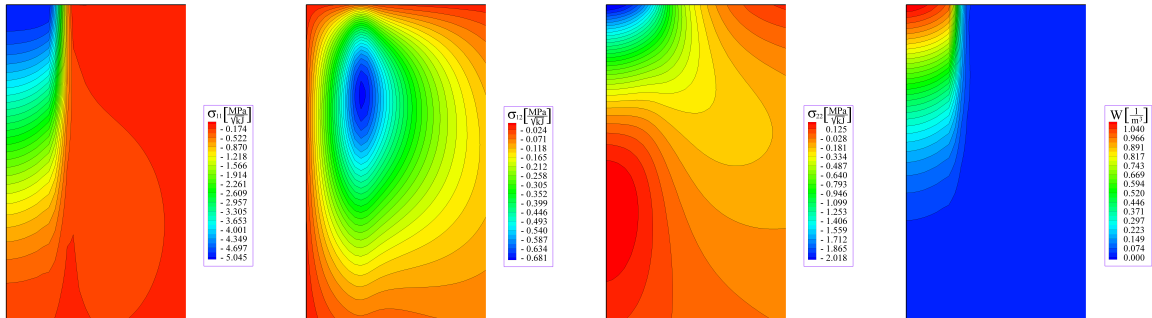
Computational results: Dynamic problem

Level curves of stresses σ_{11}, σ_{12}, σ_{22} and elastic energy W in the ground under loading platform (loading time $t_0 = 5\,ms$)

Computational results: Dynamic problem

Level curves of stresses σ_{11}, σ_{12}, σ_{22} and elastic energy W in the ground under loading platform (loading time $t_0 = 10\,ms$)

Seismograms of velocity (static loading)

Figures show the spectral curves of seismograms of the vertical velocity v_1 for **a ground** at a depth of 30 m at three points – on the axis of symmetry, on distance 15 and 30 m from this axis (red, green and blue lines).

Increasing the platform radius does not lead to a perceptible change in frequencies. The main frequency of oscillation, corresponding to the maximum amplitude of velocity, lies within $40 - 45$ Hz, which is consistent with field observations.

$r_0 = 0.57$ m $\qquad\qquad\qquad\qquad r_0 = 0.8$ m
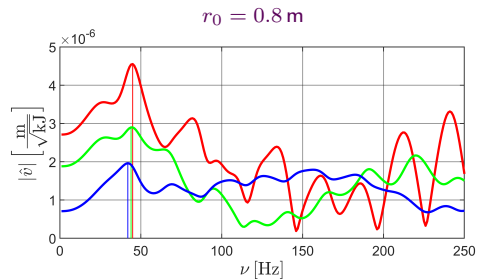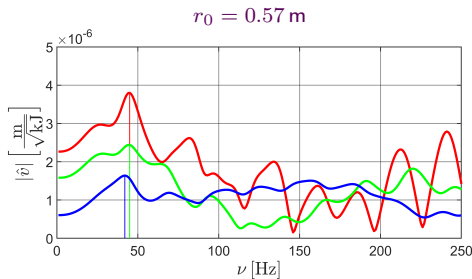
Amplitude–frequency characteristics of the velocity v_1 for a ground under static loading with instantaneous unloading

Computations were performed within the framework of the model of a static stress state with instantaneous unloading for platforms of radii $r_0 = 0.57$ and $r_0 = 0.8$ m.

Seismograms for construction of spectral curves were computed in the time interval $t^* = 0.5$ s.
Computational grid – 1000×1000 cells in spatial variables, up to 50000 layers by time.

Seismograms of velocity (static loading)

Figure shows the spectral curves of seismograms of the vertical velocity v_1 for **a rigid ground** with high velocities of longitudinal and transverse elastic waves at a depth of $30\,\mathrm{m}$ at three points – on the axis of symmetry, on distance 15 and $30\,\mathrm{m}$ from this axis (red, green and blue lines).

In this case, the characteristic frequencies of waves are about $15\,\mathrm{Hz}$ higher than in the case of a ground with lower velocities.

$$r_0 = 0.57\,\mathrm{m}$$
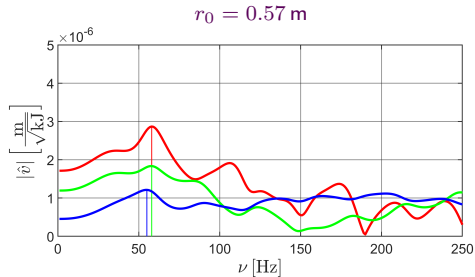
Amplitude–frequency characteristics of the velocity v_1 for a rigid ground under static loading with instantaneous unloading

Computations were performed within the framework of the model of a static stress state with instantaneous unloading for a platform of radius $r_0 = 0.57\,\mathrm{m}$.

Similar results of comparison were obtained in computations for a platform of radius $r_0 = 0.8\,\mathrm{m}$.
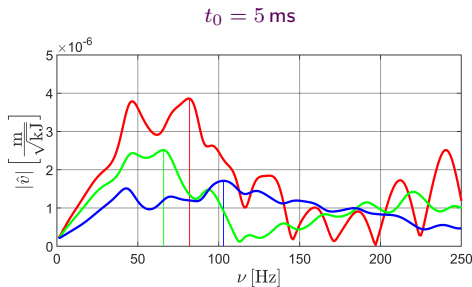
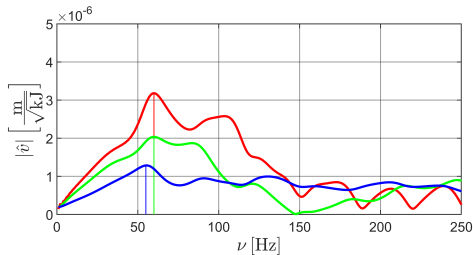# Seismograms of velocity (dynamic loading)
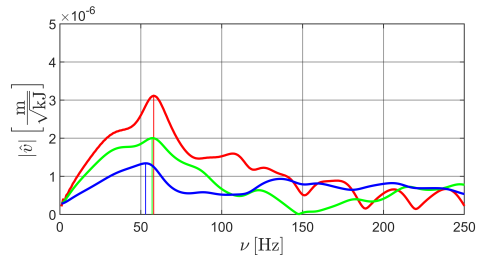
Spectral curves of seismograms of the vertical velocity v_1 in the case of pulsed loading of **a ground** through a platform of radius $r_0 = 0.57$ m with a time of monotone pressure increase $t_0 = 5$ and $t_0 = 10$ ms are represented in Figures. A depth of 30 m, seismograms at three points – on the axis of symmetry, on distance 15 and 30 m from this axis (red, green and blue lines).

The main low frequency is everywhere in the range of $40 - 45$ Hz, but at the loading time $t_0 = 5$ ms an additional peak appears with a frequency above 80 Hz, which disappears when $t_0 = 10$ ms, that is, with an increase in time of loading.

$$r_0 = 0.57 \text{ m}$$
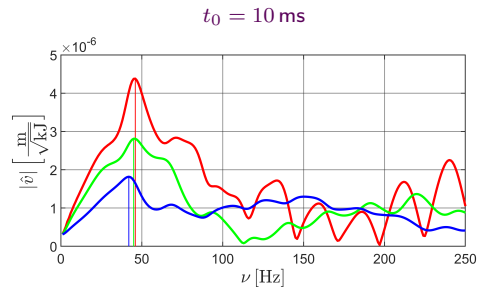
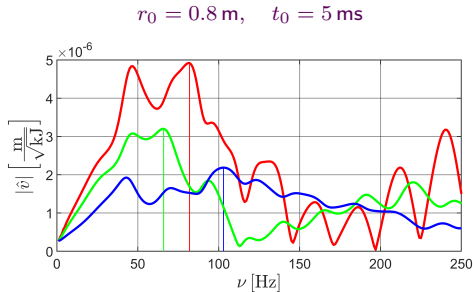*Amplitude–frequency characteristics of the velocity v_1 for a ground under dynamic loading*

Seismograms of velocity (dynamic loading)

Spectral curves of seismograms of the vertical velocity v_1 in the case of pulsed loading of **a rigid ground** through a platform of radius $r_0 = 0.57\,\text{m}$ with a time of monotone pressure increase $t_0 = 5$ and $t_0 = 10\,\text{ms}$ are represented in Figures. A depth of $30\,\text{m}$, seismograms at three points – on the axis of symmetry, on distance 15 and $30\,\text{m}$ from this axis (red, green and blue lines).

$$r_0 = 0.57\,\text{m}$$

Amplitude–frequency characteristics of the velocity v_1 for a rigid ground under dynamic loading

Seismograms of velocity (dynamic loading)

Spectral curves of seismograms of the vertical velocity v_1 in the case of pulsed loading of **a ground** through a platform of radius $r_0 = 0.8\,\text{m}$ with a time of monotone pressure increase $t_0 = 5\,\text{ms}$ are represented in Figure. A depth of $30\,\text{m}$, seismograms at three points – on the axis of symmetry, on distance 15 and $30\,\text{m}$ from this axis (red, green and blue lines).

The main low frequency is everywhere in the range of $40 - 45\,\text{Hz}$, but at the loading time $t_0 = 5\,\text{ms}$, regardless of platform radius, an additional peak appears with a frequency above $80\,\text{Hz}$, which disappears when $t_0 = 10\,\text{ms}$, that is, with an increase in time of loading.

$$r_0 = 0.8\,\text{m}, \quad t_0 = 5\,\text{ms}$$

*Amplitude–frequency characteristics of the velocity v_1
for a ground under dynamic loading*

In the considered time range, characteristic for the electromagnetic pulse source of seismic oscillations "Yenisei", the loading time influences on the amplitude–frequency characteristics of waves in the near region of a ground under a loading platform. However, this influence is not significant for the frequency corresponding to the maximum amplitude of longitudinal velocity. This frequency varies slightly depending on the loading time, on the platform radius and on the depth, and is an individual characteristic of a medium.

Thus, performed computations confirm the hypothesis of existence of the added mass and the resonant frequency of a ground.

Calculating the seismic efficiency

The computations of seismic efficiency were performed both for homogeneous and for layered ground massifs from geomaterials with different mechanical parameters.

With the same dimensions of computational domain and parameters of a spatial grid, six equidistant depth levels $h_i = 5, 10, ..., 30$ m under a platform with radii $r_i = h_i \, \mathrm{tg}\,\theta$ at a given angle θ were considered.

Geometry of the computational model is depicted in Figure.

Geometric scheme for calculating the seismic efficiency
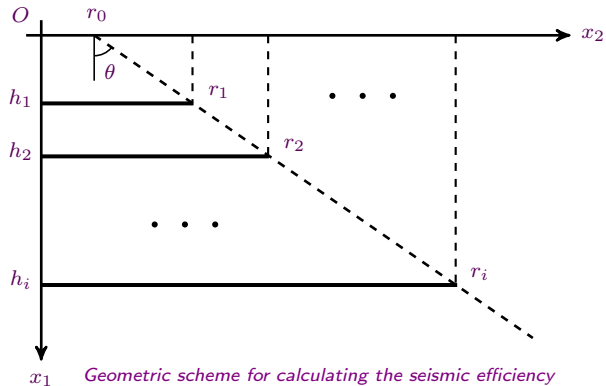
Energy fluxes

Dependences of the energy flux E_i on time in **a ground** for the angle $\theta = 45°$ are represented in Figures for two loading times. The curves for different depths h_i ($i = 1, 2, ..., 6$) are arranged in decreasing order of the energy level.

A jump-like change in the energy flux at a given depth after monotone growth occurs as the shock wave of unloading passes through corresponding area of a circle. Thereafter, the energy quickly increases to a maximum value, according to which the coefficients $æ_i$ are calculated.

A comparison of the graphs shows that a significant difference in the maximum values of the energy fluxes is observed only at small depths.

$t_0 = 5\,\text{ms}$ $t_0 = 10\,\text{ms}$
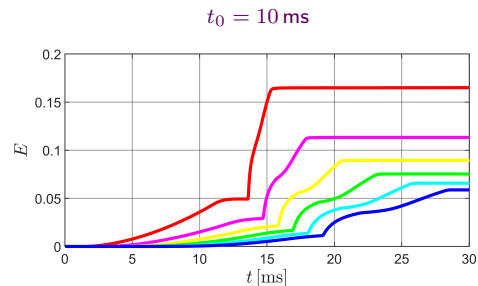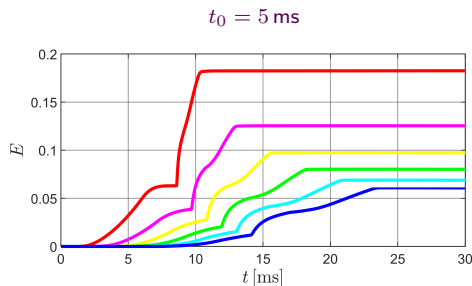
*Dependences of the energy flux E_i on time in a ground*

Seismic efficiency of a source

Dependences of efficiency æ on the angle θ at different depths for **homogeneous massifs of a ground** and **of a rigid ground** are shown in Figures.

Obtained results are in good correspondence with previous calculations for an impact source by means of the theoretical-experimental method. Some divergence of results can be explained by the features of an electromagnetic seismic source, the graph of pressure changes from which includes the initial stage of slow quasi-static loading with subsequent release of pressure.

$$t_0 = 5\,\text{ms}$$

ground
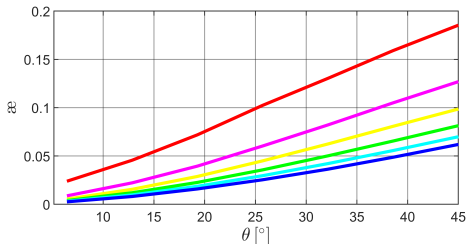
rigid ground
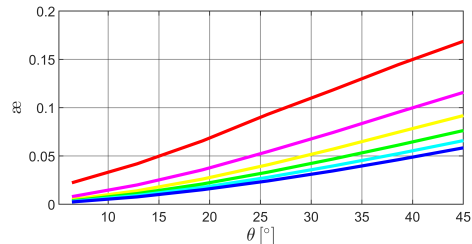
Dependences of the efficiency æ of a pulse seismic source on depth h_i and angle θ for a ground and a rigid ground
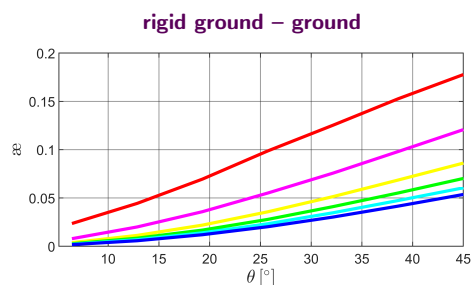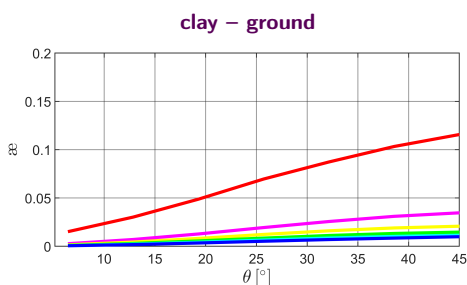
Seismic efficiency of a source

The applied method allows one to estimate the surface energy, which is obviously useless for the excitation of reflected waves. To do this, it is necessary to calculate the energy flux through a cylindrical surface of a large radius restricted by a plane at a small depth. According to computations made for a radius of $30\,\mathrm{m}$ and a depth of $0.5\,\mathrm{m}$, its share is no more than 1% of energy of a pulse action. This is the advantageous difference of the pulse seismic sources from the sources of explosive type, a significant part of whose energy is spent on the formation of shock waves in the air and on the destruction of a soil.

A 10-meter upper layer of clay above a 40-meter ground massif significantly reduces the seismic efficiency. This is because of the reflection of waves from the interface. If the upper layer above a ground consists of a rigid ground, then the seismic efficiency is about the same as in a homogeneous massif.

clay − ground $t_0 = 5\,\mathrm{ms}$ **rigid ground − ground**

Seismic efficiency æ for two-layer massifs: clay − ground, rigid ground − ground

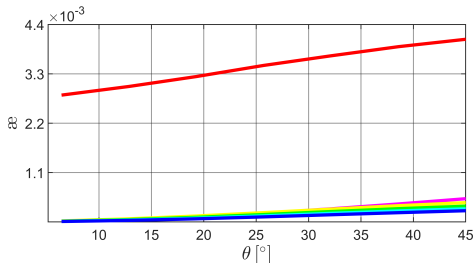# Seismic efficiency of a source

Similar computations were performed for a 10-meter reservoir of water above a ground massif, and for a 7-meter water reservoir under a 3-meter layer of ice.
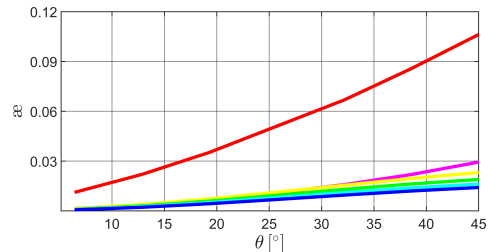
In the presence of a water barrier, the seismic efficiency of a pulse source is significantly reduced. A rigid ice layer increases the seismic efficiency, but far from indicators of homogeneous ground massifs.

$$t_0 = 5\,\text{ms}$$

Seismic efficiency æ for two-layer and three-layer massifs: water – ground, ice – water – ground

References

Sadovskii V.M., Sadovskaya O.V., Detkov V.A. **Analysis of elastic waves generated in frozen grounds by means of the electromagnetic pulse source "Yenisei". Polar Mechanics 2018. IOP Conference Series: Earth and Environmental Science**. 2018. **193**: 012058-1–012058-7.
https://iopscience.iop.org/article/10.1088/1755-1315/193/1/012058

Sadovskii V.M., Sadovskaya O.V., Efimov E.A. **Analysis of seismic waves excited in near-surface soils by means of the electromagnetic pulse source "Yenisei". Materials Physics and Mechanics**. 2019. **42**(5): 544–557.
http://mpm.spbstu.ru/no_54219/MPM542_08_sadovskii.pdf

Sadovskaya O.V., Sadovskii V.M. **Supercomputing analysis of seismic efficiency of the electromagnetic pulse source "Yenisei". AIP Conference Proceedings**. 2019. **2164**: 110011-1–110011-9.
https://aip.scitation.org/doi/10.1063/1.5130856

Sadovskii V.M., Sadovskaya O.V. **Supercomputer Modeling of Wave Propagation in Blocky Media Accounting Fractures of Interlayers.** In: **Nonlinear Wave Dynamics of Materials and Structures** (Eds.: Altenbach H., Eremeyev V.A., Pavlov I.S., Porubov A.V.). Ser.: **Advanced Structured Materials**, Vol. **122**. Springer, Cham, 2020. P. 379–398.
https://link.springer.com/chapter/10.1007/978-3-030-38708-2_22

Conclusions

- We worked out the computational technology and software complex for a detailed study of wave fields excited by the electromagnetic pulse source in blocky-layered massifs of a geomedium with different properties of layers.

- Numerical experiments shown that the developed supercomputer technology allows to reproduce with a high degree of details and accuracy in 3D setting the system of waves near the regions of excitation of seismic oscillations by a pulse source.

- Obtained results can be used in working out the optimal modes of functioning the seismic source, when mechanical characteristics of the layers vary in a wide range from solid and frozen grounds with inclusions of rock till granular and clayey water-saturated grounds.

- Numerical analysis of the wave field near the region of excitation makes also possible to obtain the averaged data, necessary for the adequate simulation of the localized pulse action from the source using simplified mathematical models for calculating the synthetic seismograms of reflected waves over large scale and at great depth of bedding inhomogeneous layers in complex geomedia.

Conclusions

- It was obtained numerically that the main frequency of vertical velocity, regardless of a material of the surface layer (clay, rigid frozen ground, water, ice-covered water), lies in the characteristic range for seismic exploration from 20 to 100 Hz.

- By means of our computational technology, quantitative characteristics of the seismic efficiency of action of a pulse source are obtained.

- Probably, improving the quality of seismic data from a pulse source can be achieved by sequential operation of electromagnets with a time interval corresponding to the frequency of resonance excitation of a geomedium.

Many thanks for your attention and for your interest!